energies

MDPI

Article

Active and Reactive Power Coordinated Optimization of Distribution Network–Microgrid Clusters Considering Three-Phase Imbalance Mitigation

Zhenhui Ouyang [1,2,*], Hao Zhong [1,2], Yongjia Wang [1,2], Xun Li [1,2] and Tao Du [1,2]

[1] College of Electrical Engineering and New Energy, China Three Gorges University, Yichang 443000, China; zhonghao022@163.com (H.Z.); 202308580121232@ctgu.edu.cn (Y.W.); 202308580121144@ctgu.edu.cn (X.L.); 17843818774@163.com (T.D.)

[2] Key Laboratory of Hubei Province for Operation and Control of Cascade Hydropower Stations, China Three Gorges University, Yichang 443002, China

* Correspondence: o15327890302@163.com

Abstract

With the continuous increase in the penetration of single-phase microgrids in low-voltage distribution networks (LVDNs), the phase asymmetry of source–load distribution has made the problem of three-phase imbalance increasingly prominent. To address this issue, this paper proposes an active–reactive power coordinated optimization model for distribution network–microgrid clusters considering three-phase imbalance mitigation. The model is formulated within a master–slave game framework: in the upper level, the distribution network acts as the leader, formulating time-of-use prices for active and reactive power based on day-ahead forecast data with the objective of minimizing operating costs. These price signals guide the flexible loads and photovoltaic (PV) inverters of the lower-level microgrids to participate in mitigating three-phase imbalance. In the lower level, each microgrid responds as the follower, minimizing its own operating cost by determining internal scheduling strategies and power exchange schemes with the distribution network. Finally, the resulting leader–follower game problem is transformed into a unified constrained model through strong duality theory and formulated as a mixed-integer second-order cone programming (MISOCP) problem, which is efficiently solved using the commercial solver Gurobi. Simulation results demonstrate that the proposed model fully exploits the reactive power compensation potential of PV inverters, significantly reducing the degree of three-phase imbalance. The maximum three-phase voltage unbalance factor decreases from 3.98% to 1.43%, corresponding to an overall reduction of 25.87%. The proposed coordinated optimization model achieves three-phase imbalance mitigation by leveraging existing resources without the need for additional control equipment, thereby enhancing power quality in the distribution network while ensuring economic efficiency of system operation.

Keywords: low-voltage distribution network; photovoltaic inverter; three-phase imbalance; distributed photovoltaics; multi-microgrid; flexible load

check for updates

Academic Editor: Tek-Tjing Lie

Received: 23 September 2025
Revised: 10 October 2025
Accepted: 17 October 2025
Published: 19 October 2025

Citation: Ouyang, Z.; Zhong, H.; Wang, Y.; Li, X.; Du, T. Active and Reactive Power Coordinated Optimization of Distribution Network–Microgrid Clusters Considering Three-Phase Imbalance Mitigation. *Energies* **2025**, *18*, 5514. https://doi.org/10.3390/en18205514

Copyright: © 2025 by the authors. Licensee MDPI, Basel, Switzerland. This article is an open access article distributed under the terms and conditions of the Creative Commons Attribution (CC BY) license (https://creativecommons.org/licenses/by/4.0/).

1. Introduction

With the rapid development of renewable energy and the large-scale integration of distributed generation, the traditional operation paradigm of distribution networks is undergoing profound transformation. As an emerging distribution network architecture, the hybrid integration of single- and three-phase microgrids has attracted significant attention

in recent years owing to its flexibility and efficiency [1–3]. By embedding single-phase microgrids into three-phase distribution networks, diverse distributed resources can be coordinated and optimally scheduled, thereby improving resource utilization efficiency and alleviating operational pressure on distribution networks. However, this transformation also poses a series of technical challenges related to the operational characteristics of hybrid single–three-phase distribution networks, including three-phase imbalance mitigation, uncertainty management of distributed energy, and optimal scheduling of flexible loads [4–6]. In this context, the coordinated operation between transmission and distribution systems is particularly important. The traditional 'passive' distribution network is gradually evolving to 'active', and the transmission system needs to share flexible resources to jointly deal with systemic problems such as voltage instability and line congestion. For example, the F-channel platform developed by Greece under the framework of 'OneNet' project in Reference [7] realizes the collaborative optimization of transmission and distribution networks in congestion management, frequency and voltage control through artificial intelligence and high-resolution weather forecast, and shows the great potential of cross-voltage level collaborative management in improving system flexibility and power quality.

At present, domestic and foreign scholars have formed a variety of technical routes in the treatment of three-phase imbalance in the distribution network, and have made remarkable progress. The existing achievements can be roughly divided into two categories: one is based on the scheme of external governance equipment. Literature [8] proposes two modes of commutation switch photovoltaic regulation and flexible load demand response to solve the problem of three-phase imbalance caused by distributed photovoltaic access, and optimize new energy consumption and reduce governance costs. Reference [9] proposed a multi-objective optimization model of active distribution network with commutation soft switching based on three-phase four-wire back-to-back voltage source converter topology. Reference [10] proposed an optimization model combining reactive power compensation devices such as on-load voltage regulating transformers and packet switching capacitors. Reference [11] proposed a three-phase four-wire DSTATCOM reference current calculation method based on PR controller and particle swarm optimization to achieve zero-sequence, harmonic and reactive power compensation, and optimize active power fluctuation control. These methods can effectively improve the three-phase balance by directly injecting compensation current or adjusting the network structure, but they usually require additional investment, and the economy needs to be improved. The second is to tap the potential of existing distributed resources, which provides a new way of thinking for the governance model. For example, reference [12] proposed a three-phase unbalance optimization method for distribution network based on iterative linearization, which uses photovoltaic inverter regulation to adjust voltage by optimizing active and reactive power output to reduce the three-phase unbalance degree of distribution network. Reference [13] proposed a voltage-reactive power coordinated control method based on low-voltage distributed photovoltaic inverters to flexibly compensate the reactive power demand of the distribution network. Reference [14] constructed a two-stage optimization model through photovoltaic phase selection switching, inverter reactive power regulation and energy storage active power regulation, which effectively reduced the three-phase unbalance and network loss of the distribution network. These studies achieve unbalanced governance by optimizing control, indicating that existing distributed resources themselves have the potential to participate in system regulation.

Although the above research has made important progress, there are still obvious limitations and room for expansion. First of all, most studies focus on centralized optimal control at the technical level, and lack effective market mechanisms and economic incentives to guide the active participation of the lower microgrid. Secondly, in terms of methodology

and research perspective, existing work, such as reference [15], focuses on data-driven black-box optimization, which is good at dealing with uncertainty but difficult to provide verifiable optimal benchmarks in deterministic scenarios. Reference [16] focused on passive safety assessment after failure, rather than pre-prevention through market mechanisms. In addition, in the study of three-phase imbalance control, the existing schemes mostly consider the regulation of active or reactive power in isolation, and fail to form a complete solution to synergistically utilize the potential of the two under the market mechanism.

In view of the above shortcomings, this paper proposes a framework for active and reactive power collaborative optimization of distribution network-microgrid group based on master-slave game and price incentive. The contribution of this paper lies in methodology, the unified MISOCP solution strategy strictly guarantees the existence and feasibility of the equilibrium solution of the game. From the perspective of research, based on 'active prevention', we guide the pre-optimization of resources by constructing a day-ahead market mechanism. On the technical mechanism, based on the master-slave relationship between the distribution network and each microgrid in the electricity market, this paper uses economic incentives to guide the power generation side of each microgrid in the lower layer to use existing resources and load side control for three-phase imbalance management. The distribution network guides the flexible load demand response of each microgrid through the active time-of-use electricity price, and guides the photovoltaic inverters of each microgrid through the reactive power price incentive to actively participate in the three-phase imbalance management. The active and reactive power collaborative optimization model of distribution network-microgrid group considering three-phase imbalance management is established. As the leader of the upper distribution network, based on the day-ahead forecast data, the active and reactive time-of-use electricity prices for the lower microgrids are formulated to minimize the operating costs. Each microgrid in the lower layer acts as a respondent, and formulates a power interaction plan and an internal scheduling scheme designed to minimize its own operating costs based on the electricity price information provided by the upper layer. Through the unified solution of the master-slave game of distribution network-multi-microgrid, the formulation and implementation of the optimal operation strategy are finally realized. Finally, the effectiveness of the proposed model is verified by simulation examples.

The structure of this paper is as follows: In the second section, the collaborative optimization framework of distribution network-microgrid group is constructed, and the master-slave game mechanism based on electricity price incentive is clarified. In the third section, a refined model of distributed resources is established, including reactive power regulation of photovoltaic inverters, flexible load demand response and multi-energy coupling constraints. In the fourth section, a unified solution method of two-level model based on strong duality theory and KKT condition is proposed, which transforms the master-slave game into a mixed integer second-order cone programming problem that can be solved efficiently. In the fifth section, the effectiveness of the model is verified by multi-scenario simulation, and the performance differences in SVG governance, flexible load response and comprehensive coordination are compared, and the influence of photovoltaic uncertainty processing is analyzed. The sixth section discusses the advantages of the proposed method in engineering applications; the seventh section summarizes the core conclusions and proposes future research directions.

2. Construction of Coordinated Optimization Framework

The distribution network employs time-of-use electricity prices for active and reactive power to guide flexible load demand response in downstream microgrids, while using inverter reactive power output to mitigate three-phase imbalance and improve power quality.

The basic structure of the system is shown in Figure 1. A, B and C are three single-phase microgrids respectively.

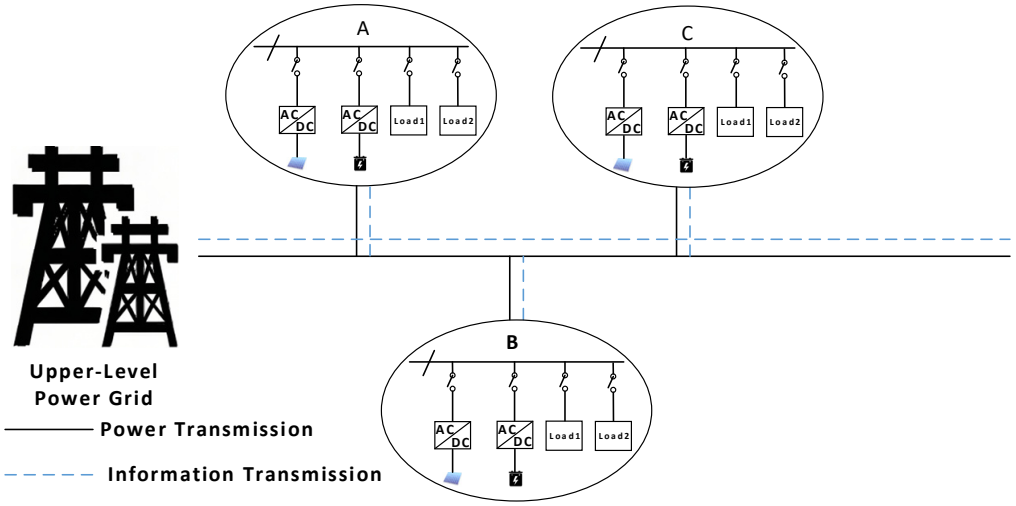


Figure 1. Basic Structure of the Distribution Network–Microgrid Cluster.

This paper proposes a coordinated active and reactive power optimization model for distribution networks with microgrid clusters, considering three-phase imbalance mitigation. First, the distribution network determines the active and reactive power prices and issues them to the downstream microgrids. Each microgrid then develops a power interaction plan with the distribution network and an internal scheduling scheme based on the information provided, and feeds the optimized power curves back to the upstream network. Next, the distribution network updates the issued active power prices and reactive power compensation prices according to the feedback from the microgrids. Finally, the entire model is optimized using a unified solution method, resulting in the formulation and implementation of the optimal operation strategy. The detailed procedure is illustrated in Figure 2.

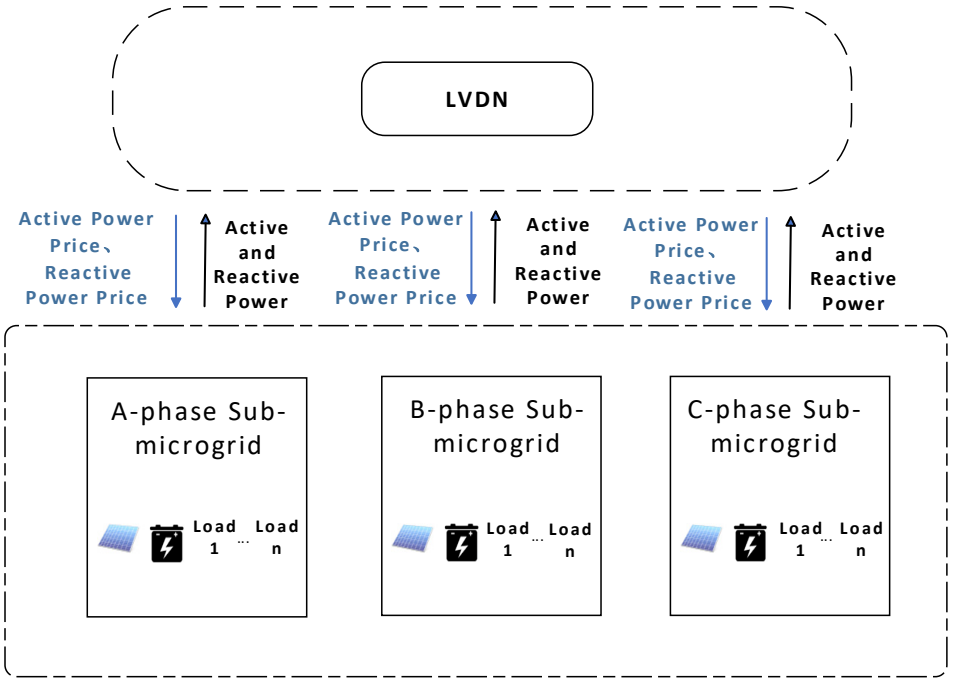


Figure 2. Leader–Follower Game Framework between the Distribution Network and Microgrids.

3. Modeling of Distributed Resources Considering Three-Phase Imbalance Mitigation

3.1. Modeling of Photovoltaic Inverters

The idle capacity of inverters in single-phase microgrid photovoltaic systems is fully utilized to provide reactive power compensation for the distribution network, enabling flexible adjustment of reactive power output and mitigation of three-phase imbalance [17–20]. The maximum reactive power output of a photovoltaic inverter is calculated as follows:

$$\begin{cases} Q_{\mathrm{PV}}^{\max} = \sqrt{S_N^2 - P_{\mathrm{PV}}^2} \\ P_{p,PV}^2(t) + Q_{p,PV}^2(t) \le S_{p,N}^2 \end{cases} \tag{1}$$

where p denotes the phase identifier, taking values from the set {A, B, C}, representing phases A, B, and C, respectively; $P_{p,PV}(t)$ represents the active power output of the PV inverter on phase pat time t; $Q_{p,PV}(t)$ represents the reactive power output of the PV inverter on phase pat time t; $S_{p,N}$ denotes the rated capacity of the inverter on phase p; P_{PV} is the rated active power of the grid-connected PV system; $Q_{\mathrm{PV}}^{\max}$ signifies the maximum reactive power output capability of the inverter.

3.2. Modeling of Flexible Loads

Flexible loads, as key controllable resources, can respond to price signals through load shifting and power curtailment. By guiding their operation with appropriately designed time-of-use electricity prices, flexible loads can not only reduce the system load peak-to-valley difference but also enhance the distribution network's capacity to accommodate distributed photovoltaic generation, thereby mitigating voltage fluctuations and three-phase imbalance to a certain extent.

(1) Price Response Characteristics of Shiftable Loads

$$\begin{cases} P_{\mathrm{tr}}^t = P_{\mathrm{tr0}}^t[1 + \varepsilon_{\mathrm{tr}}^t(\alpha_t - \alpha_t^0)/\alpha_t^0] \\ \sum\limits_{t=1}^{T} P_{\mathrm{tr0}}^t = \sum\limits_{t=1}^{T} P_{\mathrm{tr}}^t \\ \tau_t P_{\mathrm{tr}}^{\min} \le P_{\mathrm{tr}}^t \le \tau_t P_{\mathrm{tr}}^{\max} \end{cases} \tag{2}$$

where P_{tr}^t and P_{tr0}^t represent the shiftable load at node i under the dynamic electricity price and the benchmark electricity price at time t, respectively; $\varepsilon_{\mathrm{tr}}^t$ is the price elasticity coefficient of the shiftable load at node i; α_t and α_t^0 denote the electricity purchase price and the benchmark electricity price at time t, respectively; τ_t is a binary variable (0–1), where $\tau_t = 1$ indicates that the shiftable load transfer occurs at time t; $P_{\mathrm{tr}}^{\max}$ and $P_{\mathrm{tr}}^{\min}$ represent the upper and lower limits of the node power after load transfer, respectively.

(2) Price Response Characteristics of Curtailable Loads

$$\begin{cases} P_{\mathrm{cut}}^t = v_t P_{\mathrm{cut0}}^t[1 + \varepsilon_{\mathrm{cut}}^t(\alpha_t - \alpha_t^0)/\alpha_t^0] \\ \sum\limits_{t}^{t+t_{\mathrm{cut}}^{\max}} (1 - v_t) \ge 1 \\ \sum\limits_{t}^{t+t_{\mathrm{cut}}^{\min}-1} v_t \ge t_{\mathrm{cut}}^{\min}(v_t - v_{t-1}) \end{cases} \tag{3}$$

where P_{cut}^t and P_{cut0}^t represent the curtailable load at node i under the dynamic electricity price and the benchmark electricity price at time i, respectively; v_t is a binary variable (0–1), where $v_t = 1$ indicates that the curtailable load curtailment occurs at time t; $\varepsilon_{\mathrm{cut}}^t$ is the price elasticity coefficient of the curtailable load at node i; and $t_{\mathrm{cut}}^{\min}$ denote the maximum and minimum allowable duration for load curtailment, respectively.

3.3. Load and Distributed Generation Models

The injection current direction is adopted as the reference direction, and both loads and distributed generation are modeled using constant power models. The models, along with the three-phase and four-wire low-voltage distribution network (LVDN) power flow equations, are described in [14].

4. Bi-Level Optimal Scheduling Model

4.1. Distribution Network Model

4.1.1. Objective Function of the Distribution Network

The distribution network aims to minimize its own operating cost and determines the time-of-use active power prices and reactive power compensation prices for each microgrid. Its objective function is formulated as follows:

$$\min C_1 = \sum_{t=1}^{T} \left[\sum_{p=1}^{3} C^t_{\text{Grid},i,p} + \sum_{p=1}^{3} C^t_{\text{Loss},i,p} + C^t_g \right] \Delta t + \alpha f_{\text{c}} \tag{4}$$

where $p = 1, 2, 3$ correspond to phases A, B, and C, respectively; $C^t_{\text{Grid},i,p}$ represents the transaction cost between the distribution network and the microgrid at node i on phase p during time period t; $C^t_{\text{Loss},i,p}$ denotes the network loss cost associated with the microgrid at node i on phase p during time period t; C^t_g signifies the cost incurred by the distribution network for purchasing active power from the superior grid during time period t; f_{c} is the total investment cost of static var generator (SVG); α is a coefficient (value is 0 or 1), 1 is taken when SVG is installed, and 0 is taken when SVG is not installed.

(1) Cost of Purchasing Electricity from Microgrids

$$C^t_{\text{Grid},i,p} = (\delta^t_{buy,i,p} P^t_{buy,i,p} - \delta^t_{\text{sell},i,p} P^t_{\text{sell},i,p} + \delta^t_{Q,i,p} Q^t{}_{i,p}) \tag{5}$$

where $\delta^t_{buy,i,p}$, $\delta^t_{\text{sell},i,p}$, and $\delta^t_{Q,i,p}$ represent the electricity prices at which the distribution network purchases active power from, sells active power to, and purchases reactive power from the microgrid at node i on phase p during time period t, respectively; $P^t_{buy,i,p}$, $P^t_{\text{sell},i,p}$, and $Q^t{}_{i,p}$ denote the active power purchased by the distribution network from, active power sold by the distribution network to, and reactive power purchased by the distribution network from the microgrid at node i on phase p during time period t, respectively.

(2) Network Loss Cost

$$C^t_{\text{Loss},p} = \sum_{l=1}^{n-1} \sum_{p=1}^{3} P_{\text{Loss}l,p} \delta^t_{\text{sell},p} \tag{6}$$

where n represents the total number of nodes in the system network; $l = 1, 2, \cdots, n-1$ indexes the branches; $P_{\text{Loss}l,p}$ represents the power loss on phase p of branch l during time period t.

(3) Cost of Purchasing Electricity from the Superior Grid

$$C^t_g = \delta^t_p P^t_g \tag{7}$$

where δ^t_p denotes the price at which the distribution network purchases active power from the superior grid during time period t; P^t_g represents the active power purchased by the distribution network from the superior grid during time period t.

(4) Cost of SVG

The total investment cost f_c of SVG includes the investment construction cost C_{in} and the operation and maintenance cost C_{om} of SVG. The specific calculation formula is:

$$f_c = C_{in} + C_{om} \tag{8}$$

$$C_{in} = c_{SVG} \sum_{i=1}^{n} S_{SVG,i} \tag{9}$$

$$C_{om} = k_{SVG} C_{in,SVG} \tag{10}$$

where c_{SVG} represents the investment and construction cost per unit capacity of SVG; $S_{SVG,i}$ represents the installation capacity of SVG on the i th node; k_{SVG} represents the annual operation and maintenance cost coefficient of SVG.

4.1.2. Constraints

(1) Electricity Purchase and Sale Constraints

$$0 \le P^t_{buy,i,p} \le P^t_{buy,i,p,max} \tag{11}$$

$$0 \le Q^t_{buy,i,p} \le Q^t_{buy,i,p,max} \tag{12}$$

where $P^t_{buy,i,p,max}$ is the maximum value of the active power sold to the distribution network by the node i microgrid p in the period t; $Q^t_{buy,i,p,max}$ is the maximum value of reactive power sold by node i microgrid to distribution network in t period.

(2) Electricity Price Constraints

$$(1-\beta)\delta^t_f \le \delta^t_{buy,i,p} \le (1+\beta)\delta^t_f, \forall t, \forall p, \forall i \tag{13}$$

$$(1-\beta)\delta^t_f \le \delta^t_{sell,i,p} \le (1+\beta)\delta^t_f, \forall t, \forall p, \forall i \tag{14}$$

where β represents the electricity price adjustment coefficient, and its numerical range is set between 0 and 1. Based on the time-of-use electricity price of the main network, the distribution network can flexibly set the time-of-use purchase and sale electricity price for each micro-network within a certain range, so as to give full play to the incentive role of the time-of-use electricity price in guiding electricity consumption behavior.

(3) Node Voltage Constraints

$$U_{min,i} \le |U_{i,p,t}| \le U_{max,i} \tag{15}$$

where $U_{min,i}$ and $U_{max,i}$ are the minimum and maximum allowable values of node voltage, respectively. According to relevant regulations, the allowable range of voltage offset is −10%~7%.

(4) Branch Current Constraints

$$|I_{ij,t}| \le I_{max,ij} \tag{16}$$

where $I_{ij,t}$ represents the actual current carried by the branch ij at time t; $I_{max,ij}$ represents the maximum allowable current that branch ij can withstand at time t.

(5) Three-Phase Imbalance Constraints

The three-phase imbalance index f_v is defined as the sum of three-phase imbalances at the critical buses of the LVDN. It is calculated as follows:

$$f_v = \sum_{t=1}^{T} \sum_{i=1}^{n} U_{VUFi,t} \tag{17}$$

where i is the bus (node) number, and $U_{\mathrm{VUF},i,t}$ is the three-phase unbalance degree of the bus (node) i.

The formula of $U_{\mathrm{VUF},i,t}$ is:

$$U_{\mathrm{VUF},i,t} = \left| \frac{V_{\mathrm{neg},i,t}}{V_{\mathrm{pos},i,t}} \right| = \left| \frac{V_{\mathrm{a},i,t} + \alpha^2 V_{\mathrm{b},i,t} + \alpha V_{\mathrm{c},i,t}}{V_{\mathrm{a},i,t} + \alpha V_{\mathrm{b},i,t} + \alpha^2 V_{\mathrm{c},i,t}} \right| \tag{18}$$

where $V_{\mathrm{neg},i,t}$ and $V_{\mathrm{pos},i,t}$ refer to negative sequence voltage and positive sequence voltage, respectively. $V_{\mathrm{a}}, V_{\mathrm{b}}, V_{\mathrm{c}}$ are three-phase voltages of a, b and c, respectively. Parameter $\alpha = 1\angle 120^\circ$.

The three-phase imbalance of the distribution network must remain within the allowable range specified by power system operation standards, that is:

$$U_{\mathrm{VUF},i,t} \le U_{\mathrm{VUF,max}} \tag{19}$$

where $U_{\mathrm{VUF,max}}$ is the maximum allowable value of the three-phase voltage unbalance degree of the common connection point of the distribution network system, and 2% is taken according to the relevant regulations.

4.2. Microgrid Model

4.2.1. Objective Function of the Microgrid

Each microgrid, based on the active power purchase and sale prices and reactive power compensation prices set by the distribution network, aims to minimize its own operating cost and develops both the active power interaction plan with the distribution network and its internal scheduling scheme. Its objective function is formulated as follows:

$$\min C_2 = \sum_{t=1}^{n} \left[\begin{array}{l} \mathrm{C}^t_{\mathrm{w},i,p} + \mathrm{C}^t_{\mathrm{fl},i,p} + \\ C^t_{\mathrm{ESS},i,p} + \mathrm{C}^t_{\mathrm{PV},i,p} \end{array} \right] \Delta t \tag{20}$$

where $\mathrm{C}^t_{\mathrm{w},i,p}$ is the cost of purchasing electricity from the microgrid to the distribution network during the period; $\mathrm{C}^t_{\mathrm{fl},i,p}$ is the flexible load scheduling cost of the microgrid during the period; the $C^t_{\mathrm{ESS},i,p}$ and $C^t_{\mathrm{PV},i,p}$ are the energy storage and photovoltaic operating costs of the microgrid during the period, respectively.

(1) Electricity Purchase Cost

$$\mathrm{C}_{\mathrm{w},i,p} = \delta^t_{sell,i,p} P^t_{sell,i,p} - \delta^t_{buy,i,p} P^t_{buy,i,p} - \delta^t_{Q,i,p} Q^t{}_{i,p} \tag{21}$$

(2) Flexible Load Scheduling Cost

$$\mathrm{C}_{\mathrm{fl},i,p} = \sum_{t=1}^{T} \sum_{p=1}^{3} \delta^t_{fl,i,p} (P^t_{i,p,\mathrm{cut}} + P^t_{i,p,\mathrm{tr}}) \tag{22}$$

where $\mathrm{C}_{\mathrm{fl},i,p}$ represents the unit cost of the flexible load in the i-node phase microgrid; $P^t_{i,p,\mathrm{cut}}$ and $P^t_{i,p,\mathrm{tr}}$ represent the reducible and transferable load of i-node p-phase microgrid in t period, respectively.

(3) Energy Storage Operating Cost

$$C^t_{\mathrm{ESS},i,p} = w_{\mathrm{es}} \left(P^t_{\mathrm{in,i,p}} + P^t_{\mathrm{out,i,p}} \right) \tag{23}$$

where w_{es} is the operating cost coefficient of energy storage; $P^t_{\mathrm{in,i,p}}$ and $P^t_{\mathrm{out,i,p}}$ respectively represent the charging and discharging power of the energy storage of the i-node p-phase microgrid in the t-period.

(4) Photovoltaic Operating Cost

$$C_{\mathrm{PV},i,p}^{t} = w_{\mathrm{pv}} P_{\mathrm{pv,i,p}}^{t} \tag{24}$$

where w_{pv} is the operating cost coefficient of photovoltaic; $P_{\mathrm{pv,i,p}}^{t}$ is the photovoltaic output power of the i-node p-phase microgrid during the period.

4.2.2. Constraints

(1) Power Balance Constraints

$$P_{\mathrm{pv}}^{t} + P_{\mathrm{out}}^{t} + P_{buy}^{t} = P_{\mathrm{in}}^{t} + P_{sell}^{t} + P_{\mathrm{ld}}^{t} + P_{fl}^{t}, \forall t \tag{25}$$

where P_{pv}^{t} is the photovoltaic power generation in the period; P_{out}^{t} is the discharge power of energy storage in t period; P_{buy}^{t} is the power value transmitted from the distribution network to the microgrid during the t period; P_{in}^{t} is the charging power of energy storage in t period; P_{sell}^{t} is the power transmitted from microgrid to distribution network in t period; P_{ld}^{t} is the rigid load power in t period; P_{fl}^{t} is the flexible load power in t period.

(2) Energy Storage Constraints

$$\mathrm{SOC}^{t+1} = \mathrm{SOC}^{t}(1-\sigma) + \frac{\eta P_{\mathrm{in}}^{t} \Delta t}{S_{\mathrm{cap}}} - \frac{P_{\mathrm{out}}^{t} \Delta t}{\eta S_{\mathrm{cap}}} \tag{26}$$

$$\mathrm{SOC}^{1} = \mathrm{SOC}^{n+1} = \mathrm{SOC_s} \tag{27}$$

$$\mathrm{SOC_{min}} \le \mathrm{SOC}^{t} \le \mathrm{SOC_{max}}, \forall t \tag{28}$$

$$0 \le P_{\mathrm{in}}^{t} \le P_{\mathrm{in,max}}, \forall t \tag{29}$$

$$0 \le P_{\mathrm{out}}^{t} \le P_{\mathrm{out,max}}, \forall t \tag{30}$$

where SOC^{t} represents the state of charge of the energy storage system at time t; S_{cap} represents the rated capacity of the energy storage device; $\mathrm{SOC_{min}}$ and $\mathrm{SOC_{max}}$ are the minimum and maximum charges allowed by the energy storage device, respectively. $\mathrm{SOC_s}$ is the amount of charge stored in the initial moment; $P_{\mathrm{in,max}}$ and $P_{\mathrm{out,max}}$ represent the maximum charging power and the maximum discharging power of the energy storage system, respectively. σ denotes the self-discharge rate of energy storage; η denotes the charge–discharge efficiency of energy storage.

(3) Photovoltaic constraints

Considering that the PV output scheduling value is affected by its predicted output, the following constraints are imposed:

$$0 \le P_{\mathrm{pv}}^{t} = [P_{\mathrm{PV1_{dn},}t}, P_{\mathrm{PV1_{up},}t}] \tag{31}$$

The confidence level ξ is introduced to characterize the satisfaction degree of the interval number constraint. The value range of ξ is [0, 1], then P_{pv}^{t} can be expressed as:

$$P_{\mathrm{pv}}^{t} = \xi P_{\mathrm{PV1_{dn},}t} + (1-\xi) P_{\mathrm{PV1_{up},}t} \tag{32}$$

Specifically, the confidence level ξ characterizes the satisfaction degree of interval number constraints more from the possibility of interval number constraints. If the confidence level ξ is larger, the more it is necessary to ensure that the scheduling value P_{pv}^{t} is within its constraint range. It is considered that $\xi P_{\mathrm{PV1_{dn},}t} + (1-\xi) P_{\mathrm{PV1_{up},}t}$ tends to take a small value; if the smaller the confidence level A is, the less likely the interval number constraint is satisfied, and it is considered that $\xi P_{\mathrm{PV1_{dn},}t} + (1-\xi) P_{\mathrm{PV1_{up},}t}$ tends to take a large value.

5. Model Solution

The distribution network's master model and the microgrids' follower models are formulated as a leader–follower game. Due to the introduction of time-of-use pricing, the strategies and responses between the leader and followers are highly coupled. Using an iterative method may result in difficulties in ensuring convergence and global optimality. Therefore, a unified solution approach is adopted in this study. By applying strong duality theory and the Karush–Kuhn–Tucker (KKT) conditions, the lower-level responses are equivalently transformed into a set of mixed-integer linear constraints and incorporated into the master model, forming a unified modeling framework. This method effectively preserves the optimality conditions of the lower level, reconstructing the leader–follower game as a mixed-integer second-order cone programming (MISOCP) model. A commercial solver can then be used to achieve integrated solution, ensuring the existence and feasibility of the game-theoretic solution.

Unified Reformulation of the Leader–Follower Model

By applying strong duality theory, the lower-level microgrid models are transformed into mixed-integer linear constraints, which are then incorporated into the master model. Consequently, the distribution network's master model and the microgrids' leader–follower models can be unified and reformulated as a mixed-integer second-order cone programming (MISOCP) problem expressed in compact matrix form, facilitating integrated solution [21], as follows:

$$\text{obj.}C = \min_{y,z} \alpha^{\mathrm{T}} y \tag{33}$$

$$\text{s.t.} \quad Cy = g \tag{34}$$

$$Dy + Ez \leq f \tag{35}$$

$$\|Q_i y + q_i\|_2 \leq c_i^{\mathrm{T}} y + d_i \tag{36}$$

where α is the cost coefficient vector of continuous variables in the objective function; y and z represent continuous optimization variables and discrete optimization variables, respectively. Formula (29), Formula (30) and Formula (31) represent their equality constraints, inequality constraints and second-order cone constraints, respectively.

6. Example Analysis

6.1. Example Setting

The simulation in this study is conducted on a three-phase four-wire low-voltage distribution network (LVDN) whose system topology is shown in Figure 3. The length, impedance, transformer and other parameters of the distribution line are shown in Tables 1 and 2, which are taken from Reference [22], with both loads and distributed photovoltaic generation modeled as constant power. Each single-phase microgrid node is equipped with flexible loads capable of responding to control signals. The rated powers of these flexible loads are 5 kW, 4.2 kW, and 4.6 kW, respectively, with adjustable ranges up to half of their rated power. Single-phase photovoltaic (PV) units and energy storage systems are connected at buses 3, 5, and 7. The rated generation power of the single-phase PV units is 15 kW, and the inverter capacity is 1.1 times the rated active power of the PV units. The inverter cost coefficients are 3.6×10^{-6}, 0.0102, and 29.522, respectively. The energy storage systems have rated capacities of [value], with charge/discharge power limits equal to one-fourth of their rated capacity and an efficiency of 90%. The price elasticity coefficient ε is taken from the reference [23]. c_{SVG} is 200 yuan/kvar, k_{SVG} is 0.05, $S_{\mathrm{SVG},i}$ is 4 kvar. The maximum allowable three-phase voltage imbalance in the distribution network is set to 2%. The aforementioned MISOCP model is implemented in MATLAB R2014b

using the YALMIP toolbox and solved with the Gurobi 9.5.2 solver, with the optimization convergence gap set to 1%.

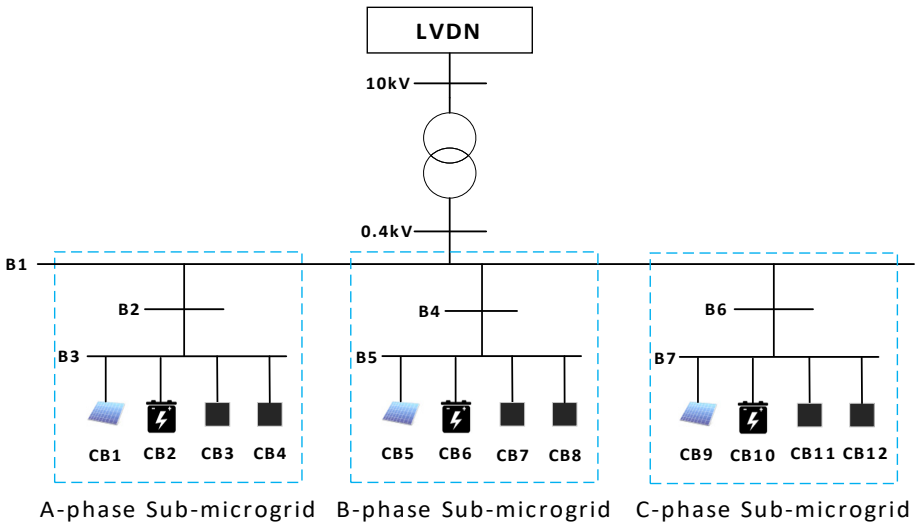


Figure 3. Low-Voltage Distribution Network Topology.

Table 1. Cable and line impedance parameters.

Type	R (Ω/km)	X (Ω/km)	B (μS/km)
N1XE-150	0.206	0.0723	40.8395
AKKJ-150	0.206	0.0628	0
EKKJ-10	1.83	0.091	100.53
AKKJ-240	0.125	0.0565	0

Table 2. Transformer parameters.

Power	500 kVA
Voltage	10/0.4 kV
Connection method	Dyn11
Positive sequence impedance	4.9%
Frequency	50 Hz

The initial electricity price information of the distribution network is presented in Table 3.

Table 3. Initial Electricity Price Information of the Distribution Network.

Scenario	Time	Active Energy Price (Yuan/(kW·h))
Peak Period	8:00–12:00, 18:00–22:00	0.83
Shoulder Period	7:00–8:00, 12:00–18:00	0.5
Off-Peak Period	0:00–7:00, 22:00–24:00	0.17

The baseline load consumption and photovoltaic generation profiles of each microgrid in the three-phase four-wire LVDN are shown in Figure 4. The load demand exhibits a clear "peak–valley–flat" pattern, which, when coordinated with the peak–valley electricity prices in Table 3, can more effectively guide users' demand response behaviors and thereby help balance the loads across the ABC phases of the distribution network.

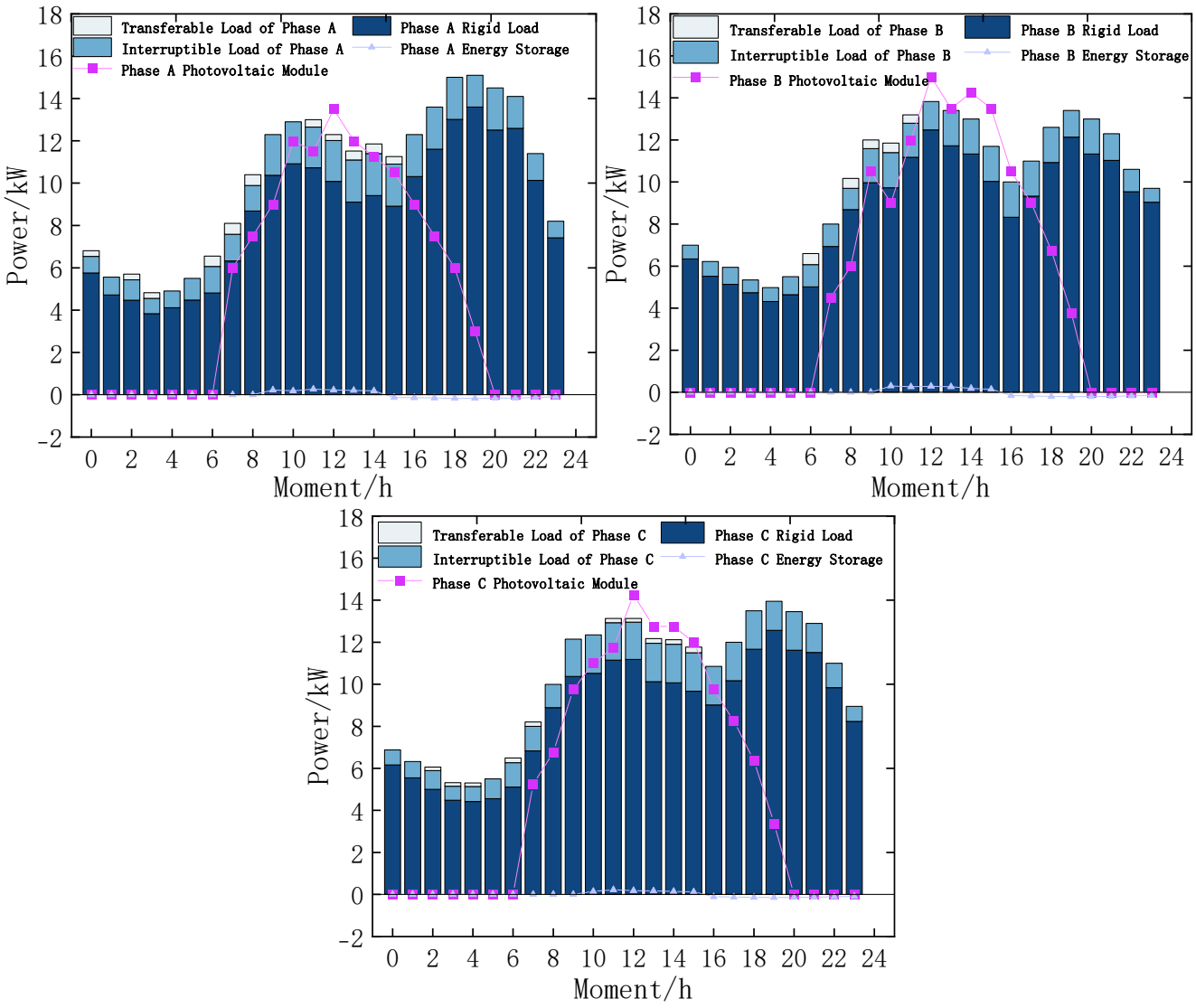


Figure 4. Load and Photovoltaic Generation Profiles of Each Microgrid.

In order to fully verify the comprehensive superiority of the collaborative optimization model proposed in this paper compared with the existing conventional governance methods, this paper sets up three typical scenarios for comparative analysis:

Three comparative scenarios are set in this study. Scenario 1: the distribution network as the main investment in the bus B2, B4, B6 installed capacity of 4 kvar SVG, with the initial load curve and fixed price (all time 0.5 yuan/(kW · h)) to optimize. Scenario 2 considers flexible load demand response, while Scenario 3 considers both flexible load demand response and the reactive power regulation capability of photovoltaic inverters. The three-phase voltage imbalance of the distribution network under these three scenarios is shown in Figure 5, and the simulation results are compared in Table 4.

Table 4. Comparison of Simulation Results.

Scenario	Comprehensive Three-Phase Imbalance/%	Maximum Three-Phase Unbalance/%
Before governance	46.10	3.98
Scenario1	21%	1.6
Scenario2	35.57	3.35
Scenario3	20.23	1.43

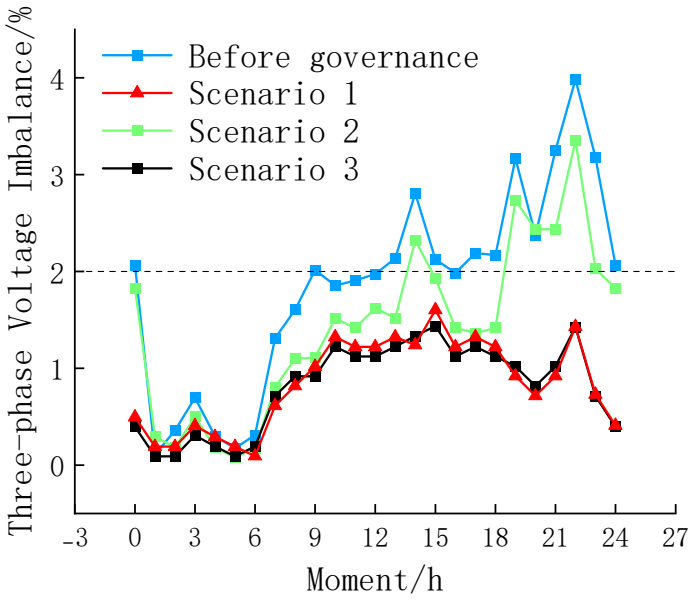


Figure 5. Three-Phase Voltage Imbalance.

6.2. Comparison of Three-Phase Voltage Imbalance

As shown in Figure 5 and Table 4, in Scenario 1, which does not consider flexible load demand response or photovoltaic (PV) inverter reactive power regulation, the three-phase voltage imbalance exhibits significant fluctuations, particularly during the morning (07:00–09:00) and evening (17:00–21:00) peak periods. The imbalance rises rapidly, reaching a maximum of 3.98%, which is well above the limit shown in the figure.

In the first scenario, that is, the distribution network as the main investment in the bus B2, B4, B6 installed capacity of 4 kvar SVG, compared with before treatment, the three-phase voltage imbalance in most of the time has been significantly improved, especially in the morning and evening peak load fluctuations, the imbalance is significantly reduced. The maximum unbalance degree decreases to about 1.6%, and the average value also decreases, indicating that SVG plays an active role in adjusting the three-phase voltage unbalance. In Scenario 2, where flexible loads participate in demand response, the distribution network sets time-of-use electricity prices based on day-ahead load forecasts. These prices guide the optimization of load profiles, prompting users to actively adjust their electricity consumption and thereby balance the three-phase load of the network. Underprice incentives, shiftable loads are transferred to off-peak periods, while curtailable loads are reduced to alleviate peak demand and lower the load peak. Compared with Scenario 1, the three-phase voltage imbalance is significantly improved in most periods, especially during the highly fluctuating morning and evening peaks, with the maximum imbalance reduced to approximately 3.35% and the average value also decreased. This indicates that flexible loads play a positive role in adjusting inter-phase load distribution and mitigating imbalance. However, although Scenario 2 partially balances load distribution across different periods and alleviates some peak-induced imbalance, the adjustment only affects active power, limiting its ability to maintain real-time dynamic voltage balance among the three phases. During periods of high PV output or concentrated asymmetric loads, significant fluctuations in voltage imbalance may still occur.

Scenario 3 further introduces the reactive power regulation capability of PV inverters. PV inverters can flexibly absorb or inject reactive power according to the voltage level of each phase, quickly adjusting node voltages and improving phase-to-phase imbalance. In this scenario, the imbalance curve is not only lower in magnitude than in the previous two scenarios but also smoother. In addition, PV inverters generate active power only

during daytime, remaining idle at night. During low-load midnight hours (00:00–06:00), the unused inverter capacity can be utilized to mitigate elevated node voltages caused by low night-time loads, thereby reducing the voltage at each microgrid and decreasing the three-phase voltage imbalance.

These results demonstrate that the proposed method does not require additional power quality equipment; the reactive power compensation capability of PV inverters alone is sufficient to manage three-phase voltage imbalance in the distribution network.

6.3. Power Output of Each Microgrid

Figures 6–8 show the active power output of single-phase sub-microgrids in each scenario. Figures 9 and 10 show the reactive power output of SVG and photovoltaic inverters in each microgrid in Scenario 1 and Scenario 2, respectively. In Scenario 1, the change trend of reactive power output of SVG is similar to that in Scenario 3. Due to the lack of effective price incentive signal, the microgrid only exchanges active power with the distribution network according to its fixed electricity demand. The flexible resources such as energy storage and reactive power capacity of photovoltaic inverters in each microgrid have not been utilized. As a whole, the microgrid has not actively participated in the three-phase unbalanced governance of the distribution network, and its output strategy is relatively single, resulting in poor overall operation economy of the system.

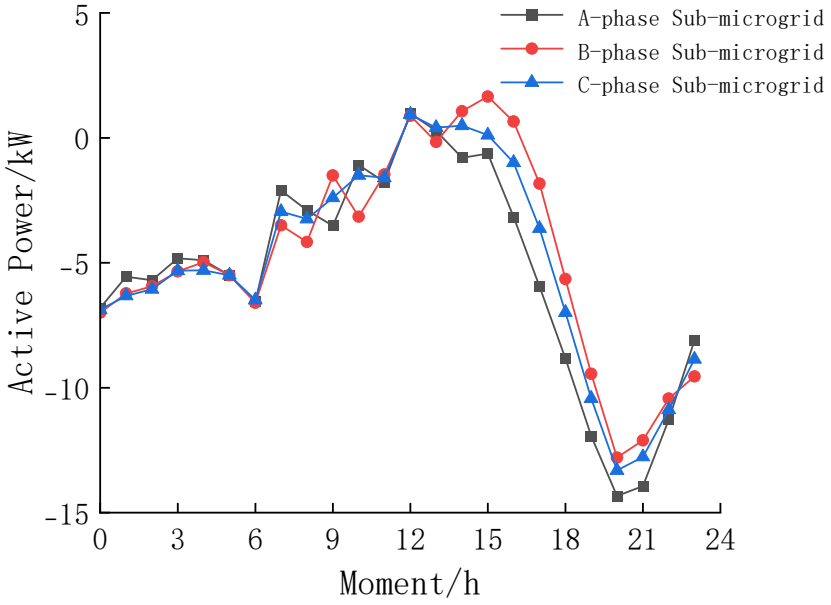


Figure 6. Active Power Purchase and Sale under Scenario 1.

In contrast, the time-of-use electricity price mechanism is introduced in Scenario 2, which makes the output behavior of each microgrid flexible. They will actively respond to the electricity price signal, reduce the load during the peak period of the electricity price or transfer it to the trough period, optimize the electricity cost of the microgrid itself, and smooth the total load curve of the distribution network by 'peak load shifting'. However, the regulation method of this scenario is limited to active power and fails to tap the potential of reactive power regulation of photovoltaic inverters, so the direct effect on improving the voltage and reactive power balance of distribution network is limited.

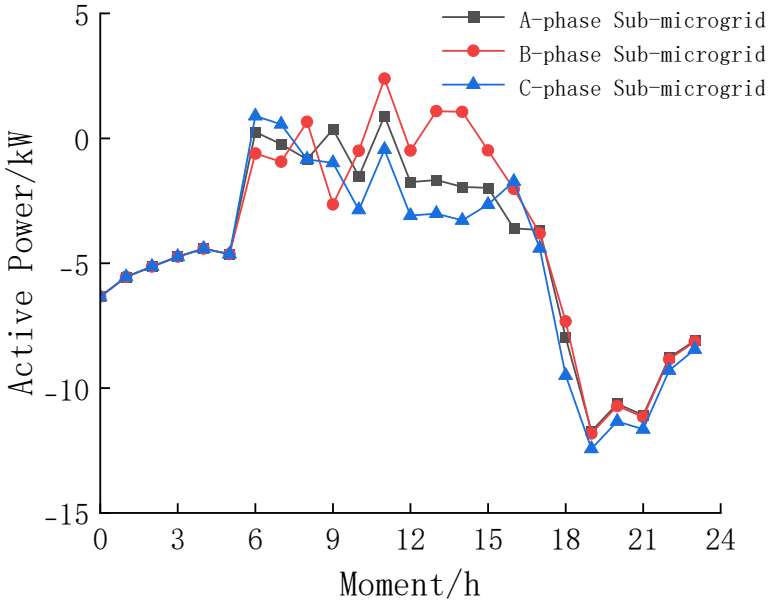


Figure 7. Active Power Purchase and Sale under Scenario 2.

In Scenario 3, from 11:00 to 14:00, the light intensity of each sub-microgrid is sufficient and there is surplus power. Part of the remaining power is stored in the battery, and the other part is sold online to maximize profits. In the rest of the time, almost all the active power is purchased from the distribution network. In the evening of the peak load period, that is, 19:00 to 22:00, the photovoltaic output power is not enough to meet the user's load demand. At this time, energy storage is used as a power supply to reduce the purchase of electricity from the grid during the peak period of electricity price, thereby improving the economy of users' electricity consumption and reducing the peak power supply pressure of the grid. However, the energy storage capacity still cannot fully meet the load demand, resulting in each sub-microgrid purchasing more active power from the distribution network, which significantly reduces the voltage of the distribution network. Since there is basically no light source to generate active power at this time, each sub-microgrid uses the idle capacity of the photovoltaic inverter to issue more reactive power to support the voltage and improve the three-phase voltage imbalance.

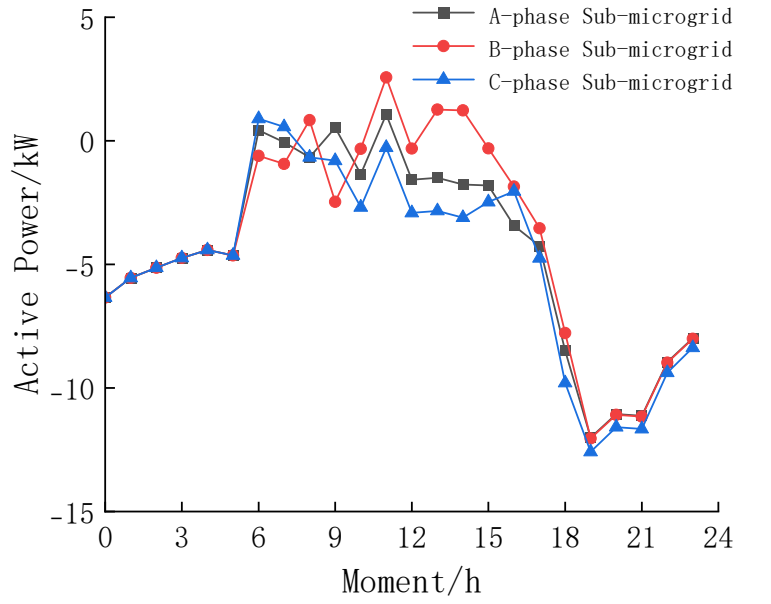


Figure 8. Active Power Purchase and Sale under Scenario 3.

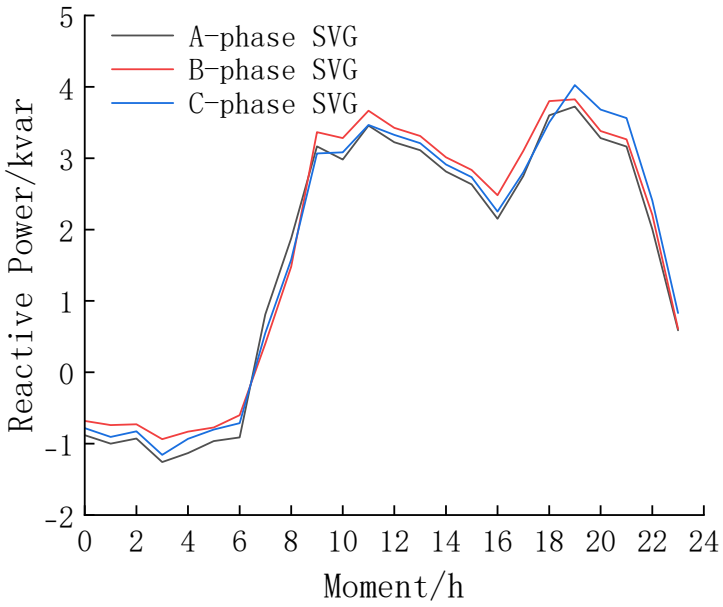


Figure 9. Scenario 1 SVG reactive power output.

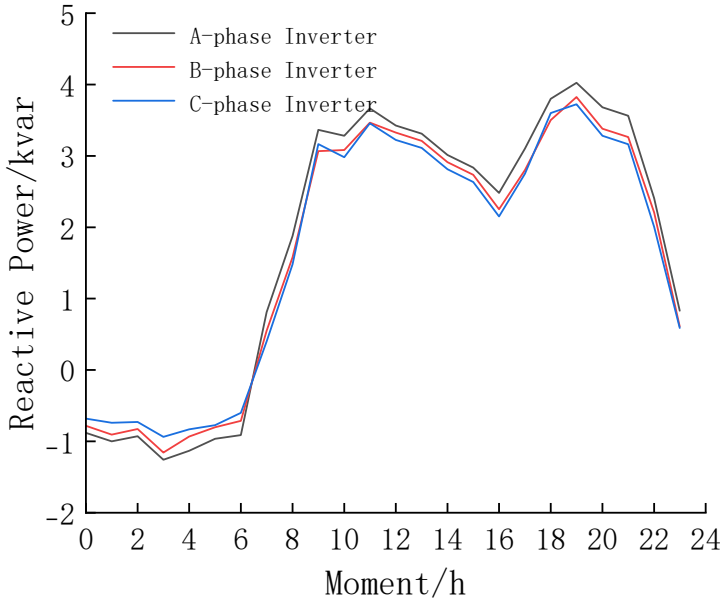


Figure 10. Inverter Power Output under Scenario 3.

It can be observed that, for the distribution network, Scenario 3 not only effectively improves power quality, but also allows each underlying microgrid to generate profit by utilizing the idle reactive power capacity of inverters to supply the distribution network.

6.4. Distribution Network Electricity Price

The electricity prices issued by the distribution network to each microgrid are shown in Figures 11 and 12, while the reactive power prices under Scenario 3 are shown in Figure 13.

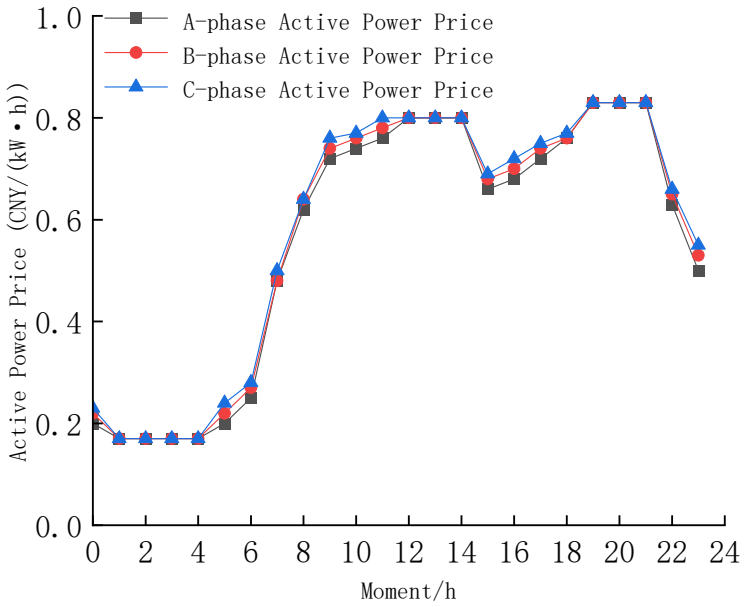


Figure 11. Active Power Electricity Price under Scenario 2.

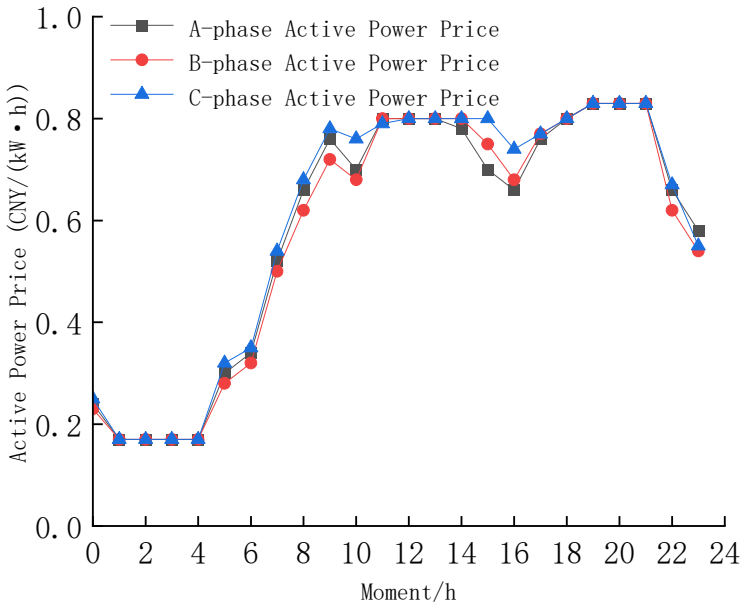


Figure 12. Active Power Electricity Price under Scenario 3.

During 01:00–05:00, the distribution network load is at its off-peak level, and the active power purchased by each microgrid is relatively low, resulting in elevated node voltages. At this time, the generation capacity of the microgrid inverters remains idle, and the reactive power prices issued by the distribution network are relatively high, incentivizing microgrids to provide reactive power to reduce voltages. During 19:00–22:00, the distribution network load reaches its peak, and the microgrids purchase a large amount of active power from the network, causing node voltages to drop and increasing the network's reactive power demand. Consequently, the reactive power prices issued to microgrids rise significantly. Although PV output is low during this period, inverters can utilize their idle capacity to provide local reactive power compensation, improving node voltage levels and reducing line currents. This not only helps mitigate three-phase voltage imbalance in the distribution network but also effectively reduces network loss costs.

From 09:00 to 15:00, PV output in the microgrids is high while loads are near peak, resulting in high inverter active power output and reduced reactive power output. Therefore, appropriate adjustment of reactive power prices is necessary to incentivize microgrids to provide reactive power compensation, balancing network losses, active and reactive power costs, and achieving an overall equilibrium between the distribution network and the underlying microgrids.

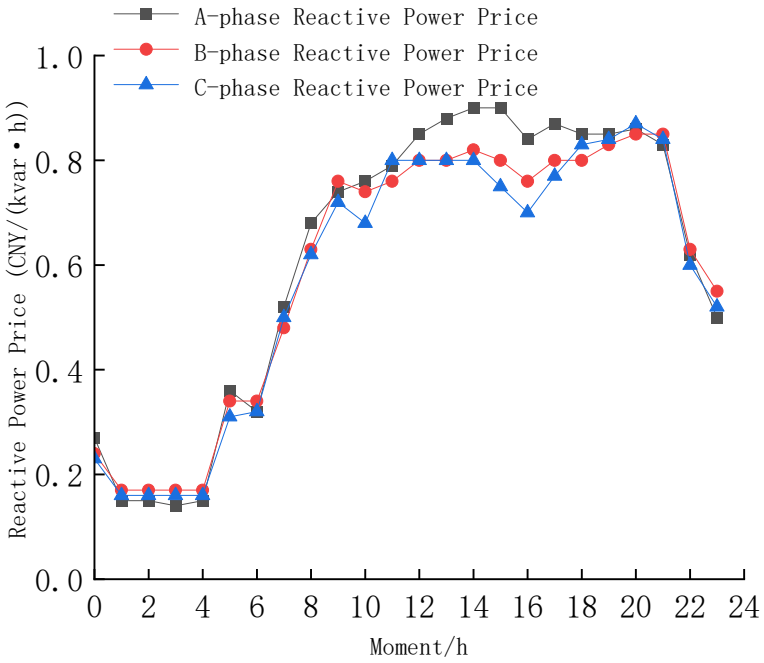


Figure 13. Reactive Power Electricity Price under Scenario 3.

6.5. Economic Analysis

6.5.1. Distribution Network Operating Cost

In Scenarios 1 and 2, the distribution network operating cost consists of the active power purchase cost from the upper-level grid and from each microgrid. In Scenario 3, the cost includes active power purchases from the upper-level grid as well as both active and reactive power purchase costs from the microgrids.

It can be seen from Table 5 that the network loss of the distribution network is reduced in Scenario 1, Scenario 2 and Scenario 3. In Scenario 1, although the distribution network can improve the power quality by installing SVG equipment, its high investment cost leads to a sharp increase in the total operating cost and poor economy. Scenario 2 only uses flexible load demand response. Although it reduces the operating cost of the distribution network, its improvement effect on network loss and imbalance is limited. In Scenario 3, in addition to introducing flexible load demand response, the reactive power regulation capability of microgrid inverters is utilized. By price incentives, microgrids provide reactive power compensation, further reducing three-phase voltage imbalance and network losses in the distribution network. This ensures that the three-phase voltage imbalance of the overall distribution network–microgrid system remains within allowable limits, thereby guaranteeing normal system operation.

Table 5. Distribution Network Operation Cost.

Scenario	Equivalent Network Loss/(kW·h)	Distribution Network Operation Cost/Yuan
Before governance	82.58	45.62
Scenario1	70.34	2452.62
Scenario2	76.96	35.45
Scenario3	60.89	31.82

6.5.2. Operating Cost of Each Microgrid

Table 6 presents the operating costs of each microgrid. It can be observed that, in Scenario 1, due to the absence of a sophisticated pricing mechanism, microgrid power purchases during peak load periods exhibit rigidity, and the energy storage system and inverter reactive power regulation capabilities are not effectively utilized, resulting in significantly reduced system economic efficiency. In Scenario 2, the introduction of flexible load demand response, guided by dynamic electricity pricing, optimizes the load profiles, encourages flexible user-side responses, and facilitates the integration of distributed PV generation, thereby reducing the operating costs of the underlying microgrids. In Scenario 3, the operating costs of the microgrids are noticeably lower than those in Scenarios 1 and 2. This is because Scenario 3 not only incorporates flexible load demand response but also employs reactive power compensation incentives to guide microgrids in fully exploiting the reactive power regulation potential of inverters, allowing microgrids to generate additional revenue and further reduce operating costs.

Table 6. Cost of Each Microgrid.

Microgrid	Scenario 1 Operating Cost/Yuan	Scenario 2 Operating Cost/Yuan	Scenario 3 Operating Cost/Yuan
A-phase sub-microgrid	64.45	65.43	40.12
B-phase sub-microgrid	56.55	56.30	32.16
C-phase sub-microgrid	59.74	68.65	45.66

6.6. The Influence of Photovoltaic Output Uncertainty Processing on the Optimization Results

The model built in this paper represents the uncertainty of photovoltaic output in the form of interval numbers, introduces the confidence level ξ to characterize the credibility of photovoltaic scheduling constraints, and converts the interval number constraints of photovoltaic output into deterministic constraints. In order to reflect the influence of confidence level change on the optimization results, combined with the above analysis, the three-phase unbalance degree of distribution network under different confidence levels is compared and simulated. The results are shown in Tables 7 and 8. It can be seen from the table that with the increase in confidence level ξ, the comprehensive three-phase unbalance degree and equivalent network loss have no obvious linear increase or decrease trend. In the engineering sense, the confidence level ξ reflects the attitude of the regional dispatcher to the photovoltaic prediction interval. The larger the ξ is, the greater the possibility of interval number constraint is, and the more it is necessary to ensure that the photovoltaic output is within the prediction range. From the perspective of mathematical theory, it is considered that the photovoltaic output is too small. In general, the uncertainty of photovoltaic output will cause uncertainty in power quality. However, combined with the results in Tables 7 and 8, it can be found that under different confidence levels ξ, the three-phase unbalance and equivalent network loss are further improved after considering the photovoltaic commutation.

Table 7. Comparison of three-phase unbalance under different confidence levels.

ξ	Three-Phase Unbalance/%
0	20.23
0.2	20.03
0.4	19.2
0.6	18.3
0.8	18.6
1	18.9

Table 8. Equivalent network loss under different confidence levels.

ξ	Equivalent Network Loss/(kW·h)
0	63.89
0.2	64.1
0.4	65.2
0.6	65.4
0.8	63.9
1	63.95

7. Discussion

In this paper, an active-reactive power collaborative optimization model of distribution network-microgrid group based on master-slave game and price incentive is proposed. The simulation results show that the model can not only effectively control the three-phase voltage imbalance within the standard without relying on additional hardware such as SVG, but also significantly improve the overall operation economy of the system, revealing the great superiority of the marketization mechanism in activating the potential of distributed resources.

Compared with the existing governance schemes, this method shows a stronger comprehensive advantage. Compared with the high investment cost of scenario 1 relying on SVG, and the limitation of scenario 2 only relying on flexible load demand response to deal with reactive power problems, the active-reactive power collaborative incentive model proposed in this paper breaks through the bottleneck of single regulation, realizes a more comprehensive mining of distributed resources, and achieves a better balance between governance effect and economy.

From the perspective of engineering application, this model provides a low-cost and high-efficiency governance path for low-voltage distribution networks with high proportion of distributed photovoltaic access. By establishing a reasonable reactive power compensation price mechanism, the lower microgrid photovoltaic inverter can be encouraged to participate in the system voltage support during the idle period, and the idle resources can be converted into adjustment capabilities. This not only improves the power quality, but also promotes the profound transformation of the distribution network operation mode from 'passive response' to 'active guidance' and 'collaborative governance' which has positive practical significance for building a new power system.

8. Conclusions and Future Work

8.1. Conclusions

This study proposes a coordinated active and reactive power optimization model for a distribution network–microgrid system, aiming to mitigate three-phase voltage imbalance in low-voltage distribution networks (LVDNs) by leveraging the reactive power

compensation capability of PV inverters and demand response from flexible loads. The main conclusions are as follows:

(1) In this method, the distribution network guides each microgrid to provide reactive power compensation services through reactive power compensation incentives. This strategy can encourage the microgrid to use its own reactive power resources and actively participate in the management of the three-phase imbalance of the distribution network, thereby improving power quality. Compared with the traditional SVG investment scheme, it can achieve the same or even better governance effect, significantly reduce the system operation cost, avoid expensive hardware investment, and show great economic advantages and application potential.

(2) Considering both flexible load demand response and the reactive power regulation capability of PV inverters, the distribution network can more precisely adjust load distribution, reduce voltage imbalance during peak periods, and further balance voltages through reactive power compensation from microgrid PV inverters, effectively reducing three-phase voltage imbalance.

(3) By implementing time-of-use pricing for active and reactive power, the distribution network can guide microgrids to participate in three-phase imbalance mitigation. Without relying on additional power quality devices, the proposed model can reduce the system's maximum three-phase voltage imbalance to 1.43% and decrease the overall imbalance by 25.87%. Through coordinated active and reactive power optimization between the distribution network and microgrids, the total system operating cost is reduced by 20.58%, significantly enhancing both power quality and economic efficiency of the distribution network–microgrid system.

8.2. Future Work

Although the model proposed in this paper has shown good results in dealing with the three-phase unbalance problem of distribution network, there are still some limitations in this study. These points also point out the direction for future research work:

(1) This paper focuses on the uncertainty of photovoltaic output and uses the interval number method to deal with it, but does not model the load fluctuation. The future research work will focus on constructing a robust scheduling strategy considering the joint uncertainty of load and renewable energy. Specifically, distributed robust optimization or data-driven stochastic programming methods can be explored to incorporate the prediction errors of load and photovoltaic into the current master-slave game framework at the same time, so as to formulate a safe and economical scheduling scheme in a more complex fluctuating environment.

(2) At present, the model in this paper is mainly oriented to the day-ahead optimization stage. An important direction in the future is to apply the proposed model to the real-time rolling optimization stage, using ultra-short-term prediction data to stabilize real-time fluctuations and achieve closed-loop optimization of decision-making. In addition, for the scenario of ultra-large-scale microgrid cluster access in the future, the current centralized solution method may face challenges, so the development of more scalable distributed algorithms will be a key research direction.

Author Contributions: Conceptualization, Z.O. and Y.W.; methodology, Z.O.; software, Z.O.; validation, Z.O.; formal analysis, Y.W.; investigation, Y.W.; data curation, H.Z.; writing—original draft preparation, H.Z.; writing—review and editing, X.L.; visualization, T.D.; Supervision, T.D. All authors have read and agreed to the published version of the manuscript.

Funding: This research was funded by Hubei Provincial Natural Science Foundation Joint Fund Project, grant number 2022CFD167.

Institutional Review Board Statement: Not applicable.

Informed Consent Statement: Not applicable.

Data Availability Statement: The data supporting the findings of this study are available from the corresponding author, Zhenhui Ouyang, upon reasonable request.

Conflicts of Interest: The authors declare no conflicts of interest.

References

1. Bian, H.; Ji, K. A Robust Collaborative Optimization of Multi-Microgrids and Shared Energy Storage in a Fraudulent Environment. *Energies* **2025**, *18*, 4635. [CrossRef]
2. Sun, H.; Zou, H.; Jia, J.; Shen, Q.; Duan, Z.; Tang, X. Master–Slave Game Optimization Scheduling of Multi-Microgrid Integrated Energy System Considering Comprehensive Demand Response and Wind and Storage Combination. *Energies* **2024**, *17*, 5762. [CrossRef]
3. Wang, X.; Wang, S.; Ren, J.; Song, Z.; Zhang, S.; Feng, H. Optimizing Economic Dispatch for Microgrid Clusters Using Improved Grey Wolf Optimization. *Electronics* **2024**, *13*, 3139. [CrossRef]
4. Feng, J.; Zhang, X.; Wang, S.; Zhao, W. ADMM-Based Two-Tier Distributed Collaborative Allocation Planning for Shared Energy Storage Capacity in Microgrid Cluster. *Electronics* **2025**, *14*, 3234. [CrossRef]
5. González-Niño, M.E.; Sierra-Herrera, O.H.; Pineda-Muñoz, W.A.; Muñoz-Galeano, N.; López-Lezama, J.M. Exploring Technology Trends and Future Directions for Optimized Energy Management in Microgrids. *Information* **2025**, *16*, 183. [CrossRef]
6. Yang, L.; Hu, Z. Implementation of Dynamic Virtual Inertia Control of Supercapacitors for Multi-Area PV-Based Microgrid Clusters. *Sustainability* **2020**, *12*, 3299. [CrossRef]
7. Zafeiropoulou, M.; Sijakovic, N.; Zarkovic, M.; Ristic, V.; Terzic, A.; Makrygiorgou, D.; Zoulias, E.; Vita, V.; Maris, T.I.; Fotis, G. Development and Implementation of a Flexibility Platform for Active System Management at Both Transmission and Distribution Level in Greece. *Appl. Sci.* **2023**, *13*, 11248. [CrossRef]
8. Shan, G.; Jie, X.; Yinghao, S.; Yi, G. Research on Three-Phase Unbalance of Distribution Networks Considering the Collaboration of Photovoltaic Phase Switching and Flexible Load. *Power Gener. Technol.* **2025**, *46*, 768–777.
9. Min, L.; Lou, C.; Yang, J. Multi-objective Operation Optimization of Active Distribution Network Considering Three-phase Unbalance Regulation of Phase-switching Soft Open Points. *Autom. Electr. Power Syst.* **2023**, *47*, 56–65.
10. Zhao, J.; Liu, X.; Lin, C.; Wei, W. Three phase Unbalanced Reactive Power Optimization for Distribution Systems with a Large Number of Single Phase Solar Generators. *Autom. Electr. Power Syst.* **2016**, *40*, 13–18.
11. Liu, F.; Gao, C.; Zhao, J. Optimization Control Strategy for DSTATCOM in Low-voltage Three-phase Unbalance Distribution Network. *Power Capacit. React. Power Compens.* **2017**, *38*, 58–63.
12. Gao, X.; Gao, Y.; Zhao, J.; Liu, X. Three-phase unbalanced optimization of a distribution network with a high proportion of distributed photovoltaic energy based on a data-driven power flow model. *Power Syst. Prot. Control.* **2024**, *52*, 77–87. [CrossRef]
13. Fu, Y.; Zhou, X.; Su, X. Adaptive and Coordinated Volt/Var Optimization for Unbalanced Active Distribution Networks of Multiple Voltage Levels. *Power Syst. Technol.* **2018**, *42*, 2136–2147. [CrossRef]
14. Chen, J.; Li, Q.; Tang, Y.; Zhang, Y. Three-phase balance optimization of low-voltage distribution network considering photovoltaic phase selection and switching. *Electr. Power Autom. Equip.* **2022**, *42*, 71–78. [CrossRef]
15. Jia, X.; Xia, Y.; Yan, Z.; Gao, H.; Qiu, D.; Guerrero, J.M.; Li, Z. Coordinated operation of multi-energy microgrids considering green hydrogen and congestion management via a safe policy learning approach. *Appl. Energy* **2025**, *401*, 126611. [CrossRef]
16. Zhang, S.; Zhang, X.; Zhang, R.; Gu, W.; Cao, G. N-1 Evaluation of Integrated Electricity and Gas System Considering Cyber-Physical Interdependence. *IEEE Trans. Smart Grid* **2025**, *16*, 3728–3742. [CrossRef]
17. Sefa, I.; Altin, N.; Ozdemir, S.; Balci, S.; Battal, F. A Novel Hybrid-Core Structure for Split-Core Inverter Output Transformers. *J. Electr. Eng. Technol.* **2025**, 1–15. [CrossRef]
18. Liu, Y.-M.; Kuo, C.-C.; Chen, H.-C. Nighttime Reactive Power Optimization for Large-Scale PV Plants: Minimizing Compensation Equipment Investment. *Appl. Sci.* **2025**, *15*, 10748. [CrossRef]
19. Liu, J.; Peng, Y.; Zhang, X.; Ning, Z.; Fan, D. Distributed Online Voltage Control with Feedback Delays Under Coupled Constraints for Distribution Networks. *Technologies* **2025**, *13*, 327. [CrossRef]
20. Tomasz, B.; Marek, N.; Stanisław, P. Power Supply and Reactive Power Compensation of a Single-Phase Higher Frequency On-Board Grid with Photovoltaic Inverter. *Energies* **2022**, *15*, 2563.
21. Fengzhou, S.; Junchao, M.; Miao, Y. A Day-ahead and Intraday Coordinated Energy Management Method for Active Distribution Networks Based on Multi-terminal Flexible Distribution Switch. *Proc. CSEE* **2020**, *40*, 778–789. [CrossRef]

22. Kim, S.P.; Song, S.G.; Park, S.J.; Kang, F.S. Imbalance Compensation of the Grid Current Using Effective and Reactive Power for Split DC-Link Capacitor 3-Leg Inverter. *IEEE Access* **2021**, *9*, 81189–81201. [CrossRef]
23. Zhao, F.; Yu, X.; Du, S.; Guo, C.; Xing, H.; Fang, Y. Assessment on flexibility of a power grid with large-scale wind farm integration considering demand response. *Power Syst. Prot. Control.* **2021**, *49*, 42–51. [CrossRef]

Disclaimer/Publisher's Note: The statements, opinions and data contained in all publications are solely those of the individual author(s) and contributor(s) and not of MDPI and/or the editor(s). MDPI and/or the editor(s) disclaim responsibility for any injury to people or property resulting from any ideas, methods, instructions or products referred to in the content.